Original Article

# Plasmonic properties of graphene-based nanostructures in terahertz waves

CrossMark

Do T. Nga [a, *], Do C. Nghia [b], Chu V. Ha [c]

[a] Institute of Physics, Vietnam Academy of Science and Technology, 10 Dao Tan, Ba Dinh, 100000 Hanoi, Viet Nam
[b] Hanoi Pedagogical University 2, Nguyen Van Linh Street, 280000 Vinh Phuc, Viet Nam
[c] Thai Nguyen University of Education, 20 Luong Ngoc Quyen, 250000 Thai Nguyen, Viet Nam

## ARTICLE INFO

## ABSTRACT

We theoretically study the plasmonic properties of graphene on bulk substrates and graphene-coated nanoparticles. The surface plasmons of such systems are strongly dependent on bandgap and Fermi level of graphene that can be tunable by applying external fields or doping. An increase of bandgap prohibits the surface plasmon resonance for GHz and THz frequency regime. While increasing the Fermi level enhances the absorption of the graphene-based nanostructures in these regions of wifi-waves. Some mechanisms for electric-wifi-signal energy conversion devices are proposed. Our results have a good agreement with experimental studies and can pave the way for designing state-of-the-art electric graphene-integrated nanodevices that operate in the GHz—THz radiation.

## 1. Introduction

Graphene has become increasingly attractive due to its unique electronic, optical and mechanical properties, as well as its various technological applications in a wide range of fields [1—3]. One of the most remarkable applications, that has drawn much attention, is graphene-based optoelectronic devices [4]. Plasmonic properties of graphene can be easily tuned through doping, the application of an external field, or the changing of temperature. Freestanding graphene in vacuum is quite transparent, having an absorption of 2.3% in the visible range. Combining other materials such as nanoparticles or biological molecules with graphene has been demonstrated to be a promising and reliable approach to enhancing the visible light absorption in graphene-based photo-detectors [5,6]. The absorbance dramatically increases in the GHz—THz regime [7]. Thus, graphene-based plasmonic devices exploit surface plasmon resonance frequencies in both visible and terahertz regimes. They have many advantages compared to the conventional plasmonic devices which use nanoscale wavelengths.

The GHz and THz bands have a broad range of applications that have been widely used in daily life and industrial business. For example, the common wifi signal is currently transmitted at GHz frequencies. However, in this era of information technology, increasingly generated data per day causes congestion for current wireless communications. The THz band can become a promising future for wireless technology since this band supports wireless terabit-per-second links [8,9]. When GHz and THz waves surround us wherever, designing plasmonic devices to take advantage of these air waves helps avoid energy waste.

In this paper, we investigate plasmonic properties of graphene-based nanostructures in the GHz and THz bands of frequency. Our findings are used to propose a theoretical model for nanodevices which converts wifi energy to electric energy based on un-derstandings of the absorption spectrum of monolayer graphene on substrates.

## 2. Theoretical background

### 2.1. Tight binding approach for graphene

Graphene is a two-dimensional material that has carbon atoms arranged in a honeycomb lattice. Let $a = 0.142$ nm be the length of the nearest-neighbor bonds. The two lattice vectors can be

---

* Corresponding author.
E-mail address: dtnga@iop.vast.ac.vn (D.T. Nga).
Peer review under responsibility of Vietnam National University, Hanoi.

expressed by $\mathbf{a}_1 = a(3/2, \sqrt{3}/2)$ and $\mathbf{a}_2 = a(3/2, -\sqrt{3}/2)$ [3]. The tight-binding Hamiltonian of electrons in graphene is given by

$$H = E_a \sum_i a_i^+ a_i + E_b \sum_i b_i^+ b_i - t \sum_{<i,j>} a_i^+ b_j - t \sum_{<i,j>} b_i^+ a_j, \quad (1)$$

where $<i,j>$ means nearest neighbors, and $a_i$ and $a_i^+$ are the annihilation and creation operator, respectively. For pure graphene, $E_a = E_b = 0$. The three nearest neighbor vectors are $\delta_1 = (1, \sqrt{3})a/2$, $\delta_2 = (1, -\sqrt{3})a/2$, and $\delta_3 = (-1,0)a$. The Hamiltonian can be rewritten by

$$H = -t \sum_i a_{\mathbf{r}_i}^+ b_{\mathbf{r}_i+\delta_1} - t \sum_i a_{\mathbf{r}_i}^+ b_{\mathbf{r}_i+\delta_2} - t \sum_i a_{\mathbf{r}_i}^+ b_{\mathbf{r}_i+\delta_3} - t$$
$$\times \sum_i b_{\mathbf{r}_i}^+ a_{\mathbf{r}_i+\delta_1} - t \sum_i b_{\mathbf{r}_i}^+ a_{\mathbf{r}_i+\delta_2} - t \sum_i b_{\mathbf{r}_i}^+ a_{\mathbf{r}_i+\delta_3}, \quad (2)$$

where $t = 2.7$ eV is the interaction potential between two nearest carbon atoms. Note that $\sum_i a_{\mathbf{r}_i}^+ b_{\mathbf{r}_i+\delta_1} = \sum_k a_k^+ b_k e^{-ik\delta_1}$.

Doing the same way with the other terms, the Hamiltonian can be recast by

$$H = \sum_k \begin{pmatrix} a_k^+ & b_k^+ \end{pmatrix} \begin{pmatrix} 0 & H_{12}(\mathbf{k}) \\ H_{21}(\mathbf{k}) & 0 \end{pmatrix} \begin{pmatrix} a_k \\ b_k \end{pmatrix}, \quad (3)$$

where $H_{12}(\mathbf{k}) = -t(e^{-ik\delta_1} + e^{-ik\delta_2} + e^{-ik\delta_3})$ and $H_{21}(\mathbf{k}) = -t(e^{ik\delta_1} + e^{ik\delta_2} + e^{ik\delta_3})$.

The Hamiltonian gives the graphene energy band

$$E_\pm(\mathbf{k}) = \pm t\sqrt{3 + f(\mathbf{k})}, \quad (4)$$

where

$$f(\mathbf{k}) = 2\cos\sqrt{3}k_y a + 4\cos\left(\frac{\sqrt{3}}{2}k_y a\right)\cos\left(\frac{3k_x a}{2}\right). \quad (5)$$

At $\mathbf{K} = (2\pi\sqrt{3}, 2\pi)/3\sqrt{3}a$ and $\mathbf{K}' = (2\pi\sqrt{3}, -2\pi)/3\sqrt{3}a$ points, $E_\pm = 0$. Near $K$ point, $\mathbf{k} = \mathbf{K} + \mathbf{q}$ with $\mathbf{q}$ relatively small, the electron energy can be calculated by

$$E_\pm = \pm\frac{3t}{2}qa. \quad (6)$$

The Hamiltonian around $K$ point can be rewritten by

$$H(\mathbf{q}) = \frac{3ta}{2}\begin{pmatrix} 0 & q_x - iq_y \\ q_x + iq_y & 0 \end{pmatrix} = v_F \hbar \boldsymbol{\sigma}\mathbf{q}, \quad (7)$$

where $v_F = 3ta/2\hbar = 10^6$ m/s is the Fermi velocity, $\boldsymbol{\sigma}$ is the Pauli matrices, and $\hbar$ is the reduced Planck constant.

## 2.2. Optical graphene conductivity

The electron density of state $|\Psi_n\rangle$ is given by

$$\rho = |\Psi_n\rangle\langle\Psi_n|, \quad (8)$$

yielding

$$\frac{d\rho}{dt} = \frac{i}{\hbar}[\rho, H]. \quad (9)$$

From Eq. (9), the fluctuation of electron density caused by an external field can be given by

$$-i\hbar\delta\dot{\rho} = [\delta\rho, H] + [\rho, \delta H]. \quad (10)$$

Suppose that $\rho \sim e^{-i\omega t}$, the above equation can be rewritten by $\hbar\omega\delta\rho = [\delta\rho, H] + [\rho, \delta H]$. From this,

$$-\hbar\omega\langle k|\delta\rho|k+q\rangle = \langle k|[\delta\rho, H]|k+q\rangle + \langle k|[\rho, \delta H]|k+q\rangle$$
$$= (E_{k+q} - E_k)\langle k|\delta\rho|k+q\rangle + (f(E_k)$$
$$- f(E_{k+q}))\langle k|\delta H|k+q\rangle, \quad (11)$$

where $f(E)$ is the Fermi distribution. The result gives

$$\langle k|\delta\rho|k+q\rangle = \frac{f(E_k) - f(E_{k+q})}{E_k - E_{k+q} - \hbar\omega}\langle k|\delta H|k+q\rangle, \quad (12)$$

Due to the external field, the electron density is fluctuated and electrons move along the direction of the field. The electrical current can be calculated by

$$\langle\delta j\rangle = Tr(\delta\rho j) = \sum_{k,q}\langle k|\delta\rho|k+q\rangle\langle k+q|j|k\rangle. \quad (13)$$

Without losing generality, it is assumed that the electrical field is along the $x$-axis. Combining Eq. (13) with Eq. (12), the current can be recast by

$$\langle\delta j_x\rangle = \sum_{k,q}\frac{f(E_k) - f(E_{k+q})}{E_k - E_{k+q} - \hbar\omega}\langle k|\delta H|k+q\rangle\langle k+q|j_x|k\rangle, \quad (14)$$

where $\delta H = -eEx$, $e$ is an electron charge, $E$ is the electric field, and the electrical current $j_x = -ev_x = -(e/\hbar)\partial H/\partial k_x = -ev_F\sigma_x$. Note that $v_x = [H,x]/(i\hbar)$.

$$\langle k|v_x|k+q\rangle = \frac{E_k - E_{k+q}}{i\hbar}\langle k|x|k+q\rangle. \quad (15)$$

Substituting Eq. (15) into Eq. (14), the graphene conductivity becomes

$$\sigma(\omega) = \sum_{k,q}\frac{f(E_k) - f(E_{k+q})}{E_k - E_{k+q} - \hbar\omega}\frac{ie^2\hbar}{E_k - E_{k+q}}\left|\langle k|v_x|k+q\rangle\right|^2$$
$$= \sigma_{intra}(\omega) + \sigma_{inter}(\omega). \quad (16)$$

For intraband transition, electrons move within a band. Thus, $|E_k - E_{k+q}| \ll k_B T$. The intra conductivity can be given by

$$\sigma_{intra}(\omega) = -\frac{2ie^2\hbar}{\hbar\omega}\sum_{k,q}\frac{\partial f(E_k)}{\partial E_k}\left|\langle k|v_x|k+q\rangle\right|^2, \quad (17)$$

where the prefactor 2 is introduced as the degeneracy of energy due to spin up and down. Note that $v_x = v_F\sigma_x$.

$$|k\rangle = \frac{1}{\sqrt{2}}\begin{pmatrix} e^{i\phi_k} \\ 1 \end{pmatrix},$$

$$\langle k|v_x|k+q\rangle = \frac{v_F}{2}\left(e^{-i\phi_k} + e^{i\phi_{k+q}}\right), \quad (18)$$

$$\left|\langle k|v_x|k+q\rangle\right|^2 = v_F^2.$$

To obtain Eq. (18), the two energy bands $E_k$ and $E_{k+q}$ are assumed to be close enough to have similar phases between the two bands $(\phi_{k+q} - \phi_k \approx 0)$. We can also introduce the damping parameter in the graphene conductivity in order to consider the damping

process on the movement of electrons in graphene. The intra conductivity is expressed by [10,11]

$$\sigma_{intra}(\omega) = \frac{2ie^2 k_B T}{\pi \hbar^2 (\omega + i\Gamma)} \ln\left[2\cosh\left(\frac{E_F}{k_B T}\right)\right], \tag{19}$$

where $E_F$ is the chemical potential of graphene and $k_B$ is the Boltzmann constant. For pristine graphene, $E_F = 0$. However, in the presence of an external field or doping, $E_F$ is nonzero and can be positive or negative [12].

The interband conductivity is caused by the transition of electrons between two bands. Thus, $|E_k - E_{k+q}| \gg k_B T$. To calculate to the interband conductivity, Eq. (16) is expanded to

$$\begin{aligned} \sigma_{inter}(\omega) &= \sum_{k,q} \frac{f(E_k) - f(E_{k+q})}{E_k - E_{k+q} - \hbar\omega} \frac{ie^2\hbar \left|\langle k|v_x|k+q\rangle\right|^2}{E_k - E_{k+q}} \\ &= \int_0^\infty \frac{v_F^2 k \, dk \, d\phi_k}{\pi^2} \frac{f(E) - f(-E)}{4E^2 - (\hbar\omega)^2} \frac{ie^2\hbar^2\omega}{E} \\ &\quad \times \left|\langle k|\sigma_x|k+q\rangle\right|^2, \end{aligned} \tag{20}$$

where the factor of 4 is due to the degeneracy of two spin states and two valleys.

$$|k\rangle = \frac{1}{\sqrt{2}}\begin{pmatrix} e^{i\phi_k} \\ 1 \end{pmatrix}, |k+q\rangle = \frac{1}{\sqrt{2}}\begin{pmatrix} -e^{i\phi_k} \\ 1 \end{pmatrix},$$
$$\langle k|\sigma_x|k+q\rangle = \frac{1}{2}\left(e^{-i\phi_k} - e^{i\phi_k}\right), \tag{21}$$
$$\left|\langle k|\sigma_x|k+q\rangle\right|^2 = \frac{1 - \cos\phi_k}{2}.$$

Now, it is easy to see that $\int_0^{2\pi}\left|\langle k|\sigma_x|k+q\rangle\right|^2 d\phi_k = \pi$. Combining Eq. (20) and Eq. (21), the interband conductivity is obtained written in the form

$$\sigma_{inter}(\omega) = \frac{ie^2\omega}{\pi}\int_0^\infty dE \frac{f(E) - f(-E)}{4E^2 - (\hbar\omega)^2}. \tag{22}$$

If the effect of the damping process is considered in calculations, $\omega \to \omega + i\Gamma$, and the interband conductivity can be recast by

$$\sigma_{inter}(\omega) = \frac{ie^2(\omega + i\Gamma)}{\pi}\int_0^\infty dE \frac{f(E) - f(-E)}{4E^2 - \hbar^2(\omega + i\Gamma)^2}. \tag{23}$$

Using the definition of the Dirac Delta function and taking the limit $\Gamma \to 0$ or $E$ very large, the real part of the interband conductivity becomes

$$\begin{aligned} Re\sigma_{inter}(\omega) &= -\frac{e^2}{2\hbar}\int_0^\infty dE[f(E) - f(-E)] \times (\delta(2E - \hbar\omega) + \delta(2E + \hbar\omega)), \\ &= \frac{e^2}{4\hbar}\frac{\sinh(\hbar\omega/2k_B T)}{\cosh(\hbar\omega/2k_B T) + \cosh(E_F/2k_B T)}, \end{aligned} \tag{24}$$

At the limit $E \gg k_B T$ or an extremely low temperature limit, $\tanh(\hbar\omega/4k_B T) \approx 1$. Thus, $Re\sigma_{inter}(\omega) = \sigma_0 = e^2/4\hbar$ is the universal conductivity of graphene which was measured in Ref. [10]. Experimental results in Ref. [10] and our theoretical calculations suggest that the imaginary part of the interband conductivity can be ignored in the considered limit.

Now, consider the optical properties of gapped graphene. The Dirac Hamiltonian is expressed by

$$H(\mathbf{k}) = \begin{pmatrix} \Delta & v_F\hbar(k_x - ik_y) \\ v_F\hbar(k_x + ik_y) & -\Delta \end{pmatrix}, \tag{25}$$

where $2\Delta$ is the gap energy between two bands. The eigenvalues of this Hamiltonian gives the energies of gapped graphene $E_\pm = \pm\sqrt{\Delta^2 + v_F^2\hbar^2 k^2}$.

$$|k\rangle = \frac{1}{\sqrt{2}}\begin{pmatrix} \sqrt{(E+\Delta)/E} \\ \sqrt{(E-\Delta)/E}e^{i\phi_k} \end{pmatrix},$$
$$|k+q\rangle = \frac{1}{\sqrt{2}}\begin{pmatrix} -\sqrt{(E-\Delta)/E}e^{i\phi_k} \\ \sqrt{(E+\Delta)/E} \end{pmatrix}. \tag{26}$$

Using the same approach for calculating the optical conductivity of pure graphene, the inter- and intra-band conductivity of gapped graphene can be obtained, [12].

$$\sigma_{intra} = \frac{ie^2/\pi\hbar^2}{\omega + i\tau^{-1}}\int_\Delta^\infty dE\left(1 + \frac{\Delta^2}{E^2}\right)[f(E) + 1 - f(-E)],$$

$$\sigma_{inter} = \frac{ie^2\omega}{\pi}\int_\Delta^\infty dE\left(1 + \frac{\Delta^2}{E^2}\right)\frac{f(E) - f(-E)}{4E^2 - \hbar^2(\omega + i\Gamma)^2}. \tag{27}$$

In all calculations, parameter $\tau = 20 \times 10^{-14}$ s and $\Gamma = 0.01$ eV for the graphene conductivity. The graphene chemical potential can be controlled by an applied electric field $E_d$ [13].

$$\frac{\pi\varepsilon_0\hbar^2 v_F^2}{e}E_d = \int_0^\infty E[f(E) - f(E + 2E_F)]dE, \tag{28}$$

where $\varepsilon_0$ is the vacuum permittivity. Eq. (28) suggests that the chemical potential $E_F = 0.2$, 0.5 and 1 eV correspond to the electric field $E_d = 0.33$, 1.918 and 7.25 V/nm, respectively. These amplitudes of the electric field larger than 5 kV/cm have been proved to cause nonlinear optical effects in graphene [14]. The nonlinear response is found to play a more important role than the linear term in the optical conductivity. In our calculations and previous studies [13], we suppose that the variation of $E_F$ is mostly due to chemical doping and the calculations using linear optical response are still valid.

## 3. Absorption of graphene

In order to estimate the absorption of graphene, the reflection and transmission coefficient of graphene on top of semi-infinite substrate must be known. These are [15,16].

$$r_{TE} = \frac{k_1 - k_2 - \mu_0\sigma(\omega)\omega}{k_1 + k_2 + \mu_0\sigma(\omega)\omega},$$
$$t_{TE} = \frac{2k_1}{k_1 + k_2 + \mu_0\sigma(\omega)\omega},$$
$$r_{TM} = \frac{\varepsilon_2 k_1 - \varepsilon_1 k_2 + \sigma(\omega)k_1 k_2/\varepsilon_0\omega}{\varepsilon_2 k_1 + \varepsilon_1 k_2 + \sigma(\omega)k_1 k_2/\varepsilon_0\omega}, \tag{29}$$
$$t_{TM} = \frac{2\varepsilon_1 k_2}{\varepsilon_2 k_1 + \varepsilon_1 k_2 + \sigma(\omega)k_1 k_2/\varepsilon_0\omega},$$

where TM and TE denote for the transverse magnetic and electric mode, respectively, $\mu_0$ is the vacuum permeability.

$k_m = \sqrt{\varepsilon_m \omega^2/c^2 - k_\parallel^2}$, $k_\parallel$ is the component of wavevector parallel to the surface, $\varepsilon_m$ is the dielectric function of medium $m$. The light comes from medium 1, partly transmits to medium 2 and reflects back into medium 1. At normal incidence, $k_\parallel = 0$

$$r_{TE} = -r_{TM} = r = \frac{\sqrt{\varepsilon_1} - \sqrt{\varepsilon_2} - \pi\alpha g(\omega)}{\sqrt{\varepsilon_1} + \sqrt{\varepsilon_2} + \pi\alpha g(\omega)},$$

$$t_{TE} = t_{TM} = t = \frac{2\sqrt{\varepsilon_1}}{\sqrt{\varepsilon_1} + \sqrt{\varepsilon_2} + \pi\alpha g(\omega)},$$
(30)

where $\alpha = 1/137$ is the fine structure constant and $g(\omega) = \sigma(\omega)/\sigma_0$. The incident and transmitted light have the intensity $I_0 = \frac{1}{2}\sqrt{\frac{\varepsilon_0}{\mu_0}}|E_0|^2 Re(\varepsilon_1)$ and $I_t = \frac{1}{2}\sqrt{\frac{\varepsilon_0}{\mu_0}}|E_t|^2 Re(\varepsilon_2)$. $E_0$ and $E_t$ are the amplitude of incident and transmitted electric fields. Thus, the absorbance of graphene can be calculated by

$$A = 1 - |r|^2 - Re\left(\frac{\sqrt{\varepsilon_2}}{\sqrt{\varepsilon_1}}\right)|t|^2.$$
(31)

For a gold substrate, the dielectric function is modeled by the Drude model [13,16].

$$\varepsilon_{Au}(\omega) = 1 - \frac{\omega_p^2}{\omega(\omega + i\gamma)},$$
(32)

where $\omega_p = 9.01$ eV is a plasma frequency of gold, and $\gamma = 0.035$ eV is the damping parameter.

For a silica substrate, the dielectric function is given by [17].

$$\varepsilon_{SiO_2}(\omega) = \varepsilon_\infty \frac{\omega_{LO}^2 - \omega^2 - i\gamma_0}{\omega_{TO}^2 - \omega^2 - i\gamma_0},$$
(33)

where $\varepsilon_\infty = 1.843$, $\omega_{LO} = 0.154$ eV, $\omega_{TO} = 0.132$ eV, and $\gamma_0 = 7.64$ meV.

## 4. Numerical results and discussions

Figure 1 presents the absorption spectra of freely-suspended graphene with a variety of chemical potentials and band gaps. The analytical expressions in previous sections show the strong dependence of absorption on the optical graphene conductivity. Thus, the intraband and interband transitions are responsible for an absorption of graphene at low and high energy regimes, respectively. In visible light regions, our results are in good agreement with Ref. [10] with $\sigma(\omega) = \sigma_0$, $A \approx \pi\alpha \approx 2.3\%$ and $T \approx 97.7\%$. Graphene is extremely transparent in air. In the GHz–THz range $\omega \ll \Gamma$, thus the $\omega$ in the denominator of Eq. (19) can be ignored. This finding suggests that $\sigma(\omega)$ and the absorption remain constant and can be significantly enhanced by increasing $E_F$. Interestingly, approximately 50% of the optical energy of the incidence light can be absorbed by graphene when $E_F = 1$ eV.

The presence of a band gap opens a once forbidden region of electron transition at energies $0 \leq \hbar\omega \leq 2\Delta$. Thus, the large band gap prevents the intraband carrier transition. As can be seen in
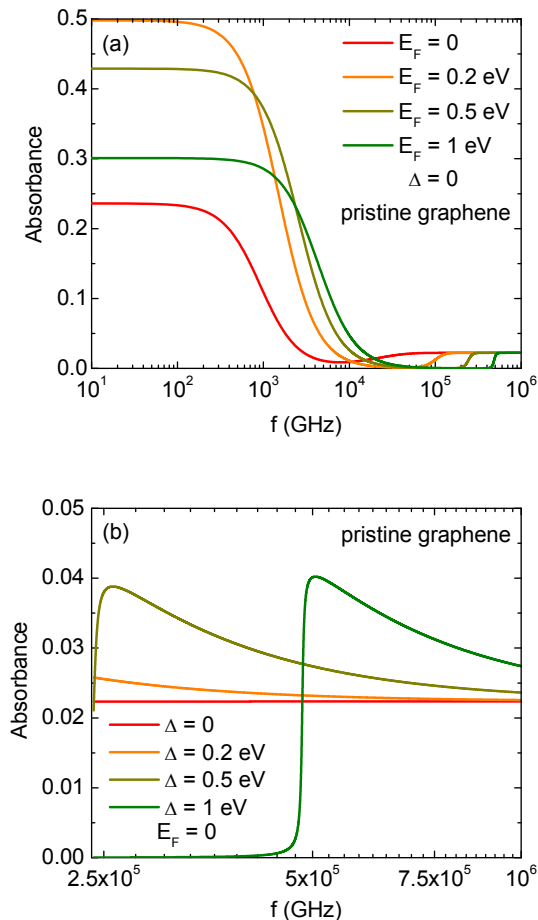


Fig. 1. Normal-incidence absorption spectra of free-standing graphene with (a) different Fermi energies when $\Delta = 0$, and (b) different values of band gap at $E_F = 0$.
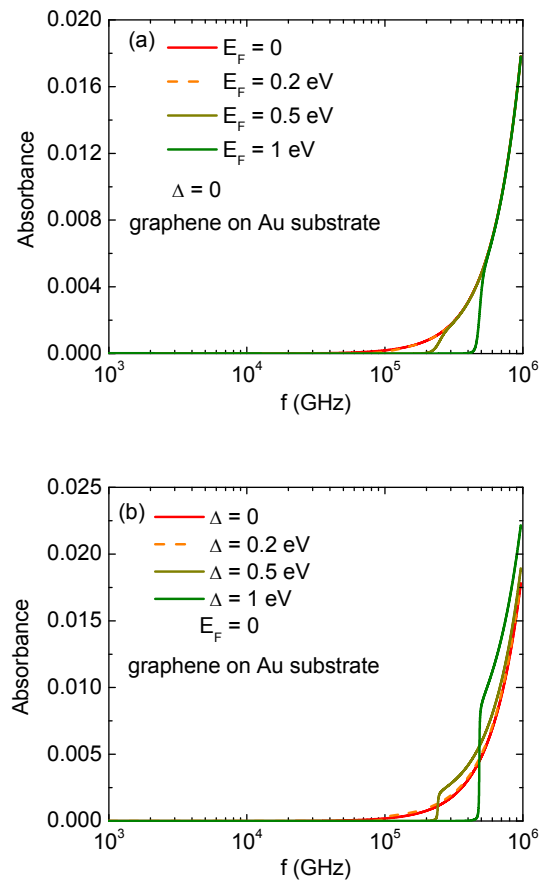


Fig. 2. Normal-incidence absorption spectra of a monolayer graphene on gold substrate with (a) different Fermi energies when $\Delta = 0$, and (b) different values of band gap at $E_F = 0$.
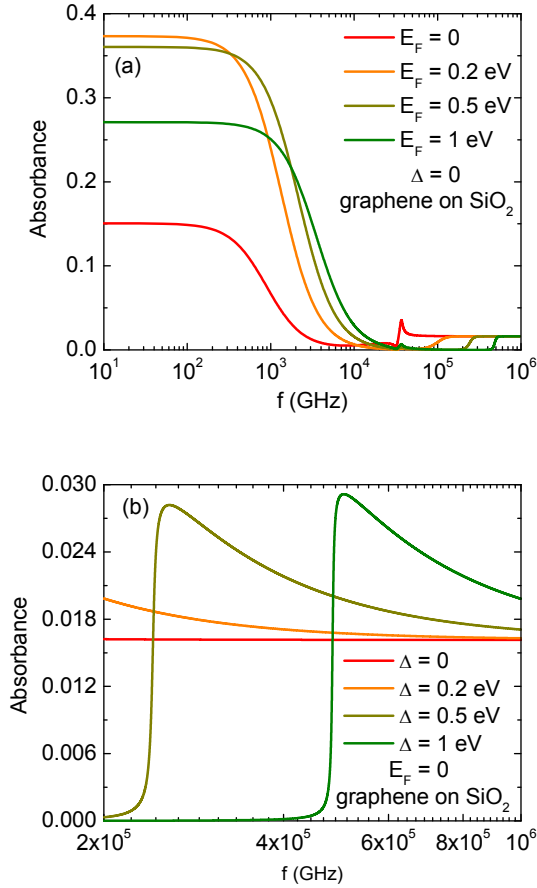
**Fig. 4.** Absorption spectrum of graphene-coated $SiO_2$ nanoparticle with $R = 50$ nm and various Fermi levels.



**Fig. 3.** Normal-incidence absorption spectra of a monolayered graphene on silica substrate with (a) different Fermi energies when $\Delta = 0$, and (b) different values of band gap at $E_F = 0$.

Fig. 1b, the absorption of graphene in the THz region is nearly zero and is only contributed to the interband conductivity.

In practice, graphene is deposited on a substrate. Thus studying the effects of substrates on graphenes optical properties is an essential key for designing graphene-based optical next-generation devices. As can be seen in Fig. 2, the absorption of graphene on gold semi-infinite substrate in air, free electrons on the gold surface absorb and re-emit the most incident photons. This result suggests that pure graphene has a higher absorption than graphene on gold substrates. $|r| \approx 1$ at low frequencies since $\varepsilon_2(\omega) \rightarrow \infty$, while
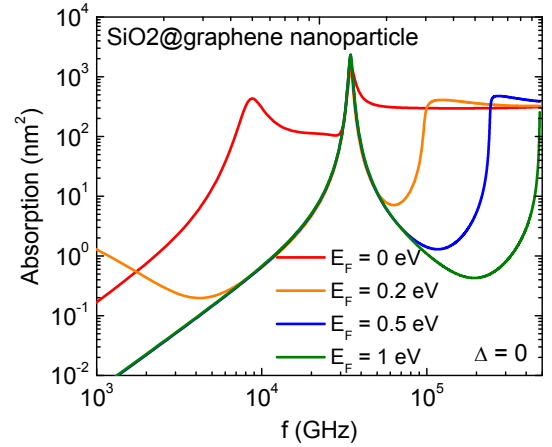
$\varepsilon_1(\omega) = 1$ and $g(\omega)$ are finite values. Total optical energy is reflected due to the presence of gold. The behavior remains regardless of variations in band gaps and Fermi energy levels. This finding also explains why the van der Waals/Casimir interactions between two planar metallic materials with and without graphene coated on top are the same [16]. Note that this dispersion force is based on the reflection of the electromagnetic field in the space separating the two objects. As a result, the plasmonic properties of graphene cannot be exploited when the substrates are metallic.

Figure 3 presents the absorption cross section of a graphene sheet on silica substrate. Silica substrates have been broadly used to support graphene sheets in many experiments and devices. Graphene on $SiO_2$ also absorbs less electromagnetic energy but the absorbance ranges from 15% to 37% as $E_F$ and $\Delta$ approach 0. Note that the nonzero bandgap induces a significant reduction of absorption at low energy. Reducing $\Delta$ as much as possible maximizes the performance of the plasmon in graphene.

Nanostructures have stronger plasmonic features than their bulk counterparts due to the quantum confinement effect. Above theoretical calculations suggest that plasmonic properties of graphene-integrated silica nanodevices may contain more interesting properties. Recently, graphene-coated dielectric nanoparticles have been intensively synthesized and investigated [18,19] for many applications with nanoparticle sizes ranging from 16 nm to 100 nm. The absorption cross section $A_{abs}$ of graphene-conjugated silica nanoparticle with a radius $R$ is given using the Mie theory [20].

$$a_l = \frac{\Psi_l\left(\frac{2\pi n_m R}{\lambda}\right)\Psi_l'\left(\frac{2\pi n_p R}{\lambda}\right) - \frac{n_p}{n_m}\Psi_l'\left(\frac{2\pi n_m R}{\lambda}\right)\Psi_l\left(\frac{2\pi n_p R}{\lambda}\right) - i\sigma\sqrt{\frac{\mu_0}{\varepsilon_0\varepsilon_m}}\Psi_l'\left(\frac{2\pi n_m R}{\lambda}\right)\Psi_l'\left(\frac{2\pi n_p R}{\lambda}\right)}{\xi_l\left(\frac{2\pi n_m R}{\lambda}\right)\Psi_l'\left(\frac{2\pi n_p R}{\lambda}\right) - \frac{n_p}{n_m}\xi_l'\left(\frac{2\pi n_m R}{\lambda}\right)\Psi\left(\frac{2\pi n_p R}{\lambda}\right) - i\sigma\sqrt{\frac{\mu_0}{\varepsilon_0\varepsilon_m}}\xi_l'\left(\frac{2\pi n_m R}{\lambda}\right)\Psi_l\left(\frac{2\pi n_p R}{\lambda}\right)},$$

$$b_l = \frac{\frac{n_p}{n_m}\Psi_l\left(\frac{2\pi n_m R}{\lambda}\right)\Psi_l'\left(\frac{2\pi n_p R}{\lambda}\right) - \Psi_l'\left(\frac{2\pi n_m R}{\lambda}\right)\Psi_l\left(\frac{2\pi n_p R}{\lambda}\right) - i\sigma\sqrt{\frac{\mu_0}{\varepsilon_0\varepsilon_m}}\Psi_l'\left(\frac{2\pi n_m R}{\lambda}\right)\Psi_l'\left(\frac{2\pi n_p R}{\lambda}\right)}{\frac{n_p}{n_m}\xi_l\left(\frac{2\pi n_m R}{\lambda}\right)\Psi_l'\left(\frac{2\pi n_p R}{\lambda}\right) - \xi_l'\left(\frac{2\pi n_m R}{\lambda}\right)\Psi_l\left(\frac{2\pi n_p R}{\lambda}\right) - i\sigma\sqrt{\frac{\mu_0}{\varepsilon_0\varepsilon_m}}\xi_l'\left(\frac{2\pi n_m R}{\lambda}\right)\Psi_l\left(\frac{2\pi n_p R}{\lambda}\right)},$$

$$A_{abs} = \frac{\lambda^2}{2\pi\varepsilon_m}\sum_{l=1}^{\infty}(2l+1)\left(Re(a_l + b_l) - |a_l|^2 - |b_l|^2\right),$$
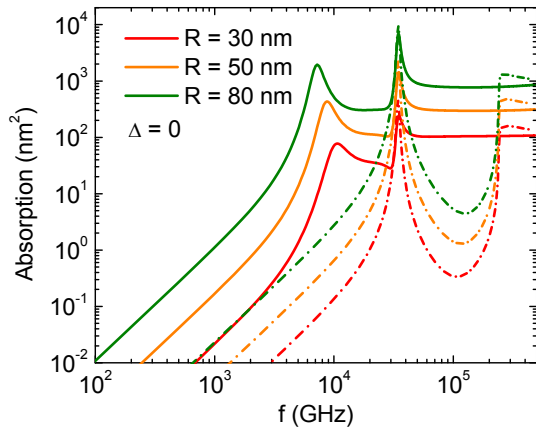
(34)

**Fig. 5.** Absorption spectrum of graphene-coated $SiO_2$ nanoparticle with $R = 30$ (red), 50 (orange) and 80 nm (green) at different chemical potentials. The solid and dashed-dotted lines correspond to $E_F = 0$ and 0.5 eV, respectively.

where $n_p = \sqrt{\varepsilon_{SiO_2}}$ is the complex refractive index of the nanoparticle, $n_m = \sqrt{\varepsilon_m} = 1$ is the refractive index of vacuum, $\Psi_l(x) = xj_l(x)$ and $\xi_l(x) = xh_l^{(1)(x)}$ are Riccati−Bessel and Riccati−Hankel functions, respectively, $j_l(x)$ is the spherical Bessel function of the first kind, and $h_l^{(1)(x)}$ is the spherical Hankel function of the first kind.

Figure 4 shows the absorption cross section of a graphene-coated 50-nm-radius $SiO_2$ nanoparticle. The Mie theory has been used to obtain predictions of theoretical calculations in good agreement with experimental results [20,21]. The full calculations of Eq. (34) are valid for all sizes of nanoparticles and wavelength range. When $\lambda \gg R$ and $\sigma = 0$, the absorption cross section can be calculated using the quasi-static approximation which only the $l = 1$ term is important. It is easy to see that two plasmonic resonances of graphene/$SiO_2$ nanoparticle are in the reliable range of the quasi-static approximation but non-zero optical conductivity of graphene layer on nanoparticle's surface leads to the failure of the approximation. Two peaks in the spectrum are attributed to the transitions of the electrons in graphene and frequencies of longitudinal and transverse optical phonons of $SiO_2$. The position of the first resonance is strongly sensitive to $E_F$ and the size of nanoparticle. The chemical potential enhancement weakens the contribution of graphene on the absorption spectrum. Technological advances have allowed the precise measuring of the particle's size. Interestingly, the absorption difference between the two optical peaks is about 1−2 orders of magnitude. This phenomenon is reversed in the bulk system.

The strong dependence of the particle size on the optical spectrum is shown in Fig. 5. The first peak resonant position is blue-shifted with increasing particle size. The magnitude of the plasmonic resonant peaks decays remarkably when the radius is reduced. The second band's position remains unchanged as varying sizes and $E_F$ of graphene since it is just dependent on phonon properties of silica. Although Fig. 3 suggests that the absorbance of graphene-coated silica substrate at low frequencies ($\leq 10^3$ GHz) is remarkably greater than that at higher frequencies, numerical results in Fig. 5 indicates that geometrical effects minify the strong low-frequency absorption. Silica@graphene nanoparticles harvest more high frequency radiation than at lower frequencies.

Certain features of the absorption spectrum in Fig. 4 can be exploited to design devices that convert the energy of GHz−THz radiation to electric energy. The coupling of the GHz−THz waves to the graphene structures results in the localized heating. The array

of these graphene nanoparticles can be designed to be illuminated by the THz band. The temperature of these particles increases and leads to electron transfer if they are connected to ground. A similar idea was experimentally carried out in a previous study [22]. Sheldon and co-workers showed that metal nanostructures can convert the visible light power to an electric potential. The plasmoelectric potential ranges from 10 to 100 mV. Thus, our proposed systems can likely obtain large plasmoelectric effects, having a wide range of applications in various fields.

## 5. Conclusion

We have studied the absorption spectrum of graphene-based systems. Graphene is quite transparent when it is put on gold substrates because the metallic substrate reflects most of the electromagnetic wave energy. The silica substrate allows approximately 15−37% incident wave energy to be absorbed on graphene. A variation of the absorbed energy depends on the Fermi energy and bandgap of graphene. The strong absorbance of graphene in the GHz−THz regime can be exterminated by increasing the bandgap. The plasmonic properties of the nanostructures are demonstrated to be much larger than that in their bulk counterparts. Two peaks in the absorption spectrum of graphene-coated silica nanoparticle can be used to produce energy converters using the plasmo-electric effect.

## References

[1] A.K. Geim, K.S. Novoselov, The rise of graphene, Nat. Mater. 6 (2007) 183−191.
[2] C. Lee, X. Wei, J.W. Kysar, J. Home, Measurement of the elastic properties and intrinsic strength of monolayer graphene, Science 321 (2008) 385−388.
[3] A.H. Castro Neto, F. Guinea, N.M.R. Peres, K.S. Novoselov, A.K. Geim, The electronic properties of graphene, Rev. Mod. Phys. 81 (2009) 109.
[4] F. Bonaccorso, Z. Sun, T. Hasan, A.C. Ferrari, Graphene photonics and opto-electronics, Nat. Photonics 4 (2010) 611−622.
[5] J. Zhu, Q.H. Liu, T. Linc, Manipulating light absorption of graphene using plasmonic nanoparticles, Nanoscale 5 (2013) 7785−7789.
[6] Y. Liu, R. Cheng, L. Liao, H. Zhou, J. Bai, G. Liu, L. Liu, Y. Huang, X. Duan, Plasmon resonance enhanced multicolour photodetection by graphene, Nat. Commun. 2 (2011) 579.
[7] O. Balci, E.O. Polat, N. Kakenov, C. Kocabas, Graphene-enabled electrically switchable radar-absorbing surfaces, Nat. Commun. 5 (2015) 6628.
[8] J. Federici, L. Moeller, Review of terahertz and subterahertz wireless communications, J. Appl. Phys. 107 (2010) 111101.
[9] R.W. McKinney, Y. Monnai, R. Mendis, D. Mittleman, A review on terahertz communications research, Terahertz Waves 32 (2011) 143−171.
[10] R.R. Nair, P. Blake, A.N. Grigorenko, K.S. Novoselov, T.J. Booth, T. Stauber, N.M.R. Peres, A.K. Geim, Fine structure constant defines visual transparency of graphene, Science 320 (2008) 1308.
[11] D. Rodrigo, O. Limaj, D. Janner, D. Etzadi, F.J.G. de Abajo, V. Pruneri, H. Altug, Fine structure constant defines visual transparency of graphene, Science 349 (2015) 165−168.
[12] J.M. Dawlaty, S. Shivaraman, J. Strait, P. George, M. Chandrashekhar, F. Rana, M.G. Spencer, D. Veksler, Y. Chen, Measurement of the optical absorption spectra of epitaxial graphene from terahertz to visible, Appl. Phys. Lett. 93 (2008) 131905.
[13] A.D. Phan, N.A. Viet, N.A. Poklonski, L.M. Woods, C.H. Le, Interaction of a graphene sheet with a ferromagnetic metal plate, Phys. Rev. B 86 (2012) 155419.
[14] S. Gong, T. Zhao, M. Sanderson, M. Hu, R. Zhong, X. Chen, P. Zhang, C. Zhang, S. Liu, Transformation of surface plasmon polaritons to radiation in graphene in terahertz regime, Appl. Phys. Lett. 106 (2015) 223107.
[15] R. Messina, P. Ben-Abdallah, Graphene-based photovoltaic cells for near-field thermal energy conversion, Sci. Rep. 3 (2013) 1383.
[16] A.D. Phan, L.M. Woods, D. Drosdoff, I.V. Bondarev, N.A. Viet, Temperature dependent graphene suspension due to thermal Casimir interaction, Appl. Phys. Lett. 101 (2012) 113118.

[17] M. Badioli, A. Woessner, K.J. Tielrooij, S. Nanot, G. Navickaite, T. Stauber, F.J.G. de Abajo, F.H.L. Koppens, Phonon-mediated mid-infrared photoresponse of graphene, Nano Lett. 14 (2014) 6374–6381.

[18] I.H. Son, J.H. Park, S. Kwon, S. Park, M.H. Rummeli, A. Bachmatiuk, H.J. Song, J. Ku, J.W. Choi, J. Choi, S.-G. Doo1, H. Chang, Silicon carbide-free graphene growth on silicon for lithium-ion battery with high volumetric energy density, Nat. Commun. 6 (2015) 7393.

[19] W. Luo, S. Zafeiratos, Graphene-coated ZnO and SiO$_2$ as supports for CoO nanoparticles with enhanced reducibility, Chem. Phys. Chem. 17 (2016) 3055–3061.

[20] C.F. Bohren, D.R. Huffman, Absorption and Scattering of Light by Small Particles, 1998.

[21] Anh D. Phan, Trinh X. Hoang, Thi H.L. Nghiem, Lilia M. Woods, Surface plasmon resonances of protein-conjugated gold nanoparticles on graphitic substrates, Appl. Phys. Lett. 103 (2013) 163702.

[22] M.T. Sheldon, J. van de Groep, A.M. Brown, A. Polman, H.A. Atwater, Plasmoelectric potentials in metal nanostructures, Science 346 (2014) 828–831.